

Suppressing TGF β signaling in regenerating epithelia in an inflammatory microenvironment is sufficient to cause invasive intestinal cancer

メタデータ	言語: eng 出版者: 公開日: 2017-10-05 キーワード (Ja): キーワード (En): 作成者: メールアドレス: 所属:
URL	http://hdl.handle.net/2297/41370

Suppressing TGF- β signaling in regenerating epithelia in an inflammatory microenvironment is sufficient to cause invasive intestinal cancer

Hiroko Oshima¹, Mizuho Nakayama^{1,2}, Tae-Su Han^{1,2}, Kuniko Naoi¹, Xiaoli Ju¹, Yusuke Maeda¹, Sylvie Robine³, Kiichiro Tsuchiya⁴, Toshiro Sato⁵, Hiroshi Sato⁶, Makoto Mark Taketo⁷, and Masanobu Oshima¹

¹Division of Genetics, Cancer Research Institute, Kanazawa University, Kanazawa, Japan;

²Core Research for Evolutional Science and Technology (CREST), the Japan Science and Technology Agency, Tokyo, Japan; ³Equipe de Morphogenese et Signalisation cellulaires, Institut Curie, Paris, France; ⁴Department of Advanced Therapeutics for Gastrointestinal Disease, Graduate School Tokyo Medical and Dental University, Tokyo, Japan; ⁵Department of Gastroenterology, Keio University School of Medicine, Tokyo, Japan; ⁶Division of Virology and Oncology, Cancer Research Institute, Kanazawa University, Kanazawa, Japan;

⁷Department of Pharmacology, Kyoto University Graduate School of Medicine, Kyoto, Japan

Running title: Invasion by TGF- β blocking in regenerating inflamed mucosa

Keywords: TGF β ; invasion; inflammation; regeneration; ulcerative colitis

Grant Support: This work was supported by CREST, the Japan Science and Technology Agency, Japan (M. Oshima), Grants-in-Aid for Scientific Research on Innovative Areas from the Ministry of Education, Culture, Sports, Science and Technology of Japan #22114005 (M. Oshima), #24300325 (M. Oshima), and Takeda Science Foundation, Japan (H. Oshima and M. Oshima).

Corresponding Author: Masanobu Oshima, Division of Genetics, Cancer Research Institute, Kanazawa University, Kanazawa, 920-1192 Japan.

Phone: 81-76-264-6760, FAX: 81-76-234-4519

E-mail: oshimam@staff.kanazawa-u.ac.jp

Disclosure of Potential Conflict of Interest: The authors disclose no potential conflicts of interest.

Word count (excluding references): 4,992

Total number of figures: 7

Abstract

Genetic alterations in the TGF β signaling pathway in combination with oncogenic alterations lead to cancer development in the intestines. However, the mechanism(s) of TGF β signaling suppression in malignant progression of intestinal tumors has not yet fully understood. We have examined *Apc*^{A716} *Tgfr2*^{ΔIEC} compound mutant mice that carry mutations in *Apc* and *Tgfr2* genes in the intestinal epithelial cells. We found inflammatory microenvironment only in the invasive intestinal adenocarcinomas but not in non-invasive benign polyps of the same mice. We thus treated simple *Tgfr2*^{ΔIEC} mice with dextran sodium sulfate (DSS) that causes ulcerative colitis. Importantly, these *Tgfr2*^{ΔIEC} mice developed invasive colon cancer associated with chronic inflammation. We also found that TGF β signaling is suppressed in human colitis-associated colon cancer cells. In the mouse invasive tumors, macrophages infiltrated and expressed MT1-MMP, causing MMP2 activation. These results suggest that inflammatory microenvironment contributes to submucosal invasion of TGF β signaling-repressed epithelial cells through activation of MMP2. We further found that regeneration was impaired in *Tgfr2*^{ΔIEC} mice for intestinal mucosa damaged by DSS treatment or X-ray irradiation, resulting in the expansion of undifferentiated epithelial cell population. Moreover, organoids of intestinal epithelial cells cultured from irradiated *Tgfr2*^{ΔIEC} mice formed 'long crypts' in Matigel, suggesting acquisition of an invasive phenotype into extracellular matrix. These results, taken together, indicate that a simple genetic alteration in TGF β signaling pathway in the inflamed and regenerating intestinal mucosa can cause invasive intestinal tumors. Such a mechanism may play a role in the colon carcinogenesis associated with inflammatory bowel disease in humans.

Introduction

Accumulating evidence indicates that inflammatory responses play an important role in cancer development (1, 2). The disruption of genes encoding cyclooxygenase 2 (COX-2) or prostaglandin E₂ (PGE₂) receptor, EP2, in *Apc*^{A716} knockout mice results in significant suppression of intestinal polyposis (3, 4). Moreover, blocking transcription factors NF-κB and Stat3 in a chemically-induced colitis-associated colon tumor model in mice causes suppression of colon tumor development (5-7). These results indicate that activation of inflammatory pathways through PGE₂, NF-κB and Stat3 is required for intestinal tumorigenesis. However, it has not yet been elucidated what role the inflammatory responses play in the progression of benign intestinal tumors to invasive adenocarcinomas.

Most intestinal adenomas are induced by *APC* mutations, resulting in the Wnt signaling activation, and tumors progress to adenocarcinomas by additional mutations such as those encoding RAS or transforming growth factor β (TGFβ) type II receptor (TGFβRII) (8). Mouse genetic studies have indicated that suppression of TGFβ signaling accelerates development of malignant intestinal tumors in combination with mutations in *Kras* or *Pten*, although TGFβ suppression alone does not cause tumorous changes (9, 10). These results indicate that suppression of the TGFβ signaling is a key process involved in the malignant progression.

The TGFβ ligand binds TGFβRII, followed by the activation of TGFβRI. Activated TGFβRI then phosphorylates Smad2/3, which causes their binding with Smad4, and the Smad complex induces transcription of TGFβ target genes (11). We have previously shown that immature myeloid cells (iMCs) are recruited and express matrix metalloproteinase 2 (MMP2) at the invasion front of compound *Apc*^{A716} *Smad4* knockout mouse intestinal

adenocarcinomas, which contribute to their submucosal invasion (12,13). Moreover, disruption of *Tgfb2*, encoding TGF β RII, in mouse mammary tumor cells results in the recruitment of myeloid cells into tumor tissues, which promotes tumor metastasis through a process involving metalloproteinase activation (14). These results indicate that suppression of TGF β signaling generates a microenvironment that is critical for progression of intestinal tumors. However, it is not understood how the inflammatory responses affect the tumor progression induced by TGF β suppression. Moreover, it has not been elucidated whether TGF β -suppressed epithelial cells acquire an invasive phenotype in tumor tissues.

We herein show that ulcerative colitis causes submucosal invasion of *Tgfb2*-disrupted intestinal epithelia, leading to the development of invasive colon cancer. Moreover, TGF β signaling suppression in regenerating epithelia caused long crypt formation in Matrigel, which may reflect an increased capacity for invasion. We also found that TGF β signaling is suppressed in human colitis-associated colon cancer cells. These results provide a novel mechanism for the development of invasive colon cancer where TGF β signaling suppression, chronic inflammation and the regeneration of epithelial cells are compounded.

Materials and Methods

Animal models

Wild-type C57BL/6 mice were purchased from CLEA (Osaka, Japan). Apc^{A716} mice, $Tgfb2^{flox/flox}$ mice, and villin-CreER mice have been described previously (15-17). $Tgfb2^{flox/flox}$ mice were obtained from Mouse Repository (NCI-Frederick, Strain Number: 01XN5, Frederick, MD). All animal experiments were carried out according to the protocol approved by the Committee on Animal Experimentation of Kanazawa University, Japan.

Animal experiments

$Apc^{A716} Tgfb2^{flox/flox}$ villin-CreER mice were treated with tamoxifen (Tmx) at 4 mg/mouse once a week, from five weeks of age to generate $Apc^{A716} Tgfb2^{AIEC}$ mice. Intestinal tumors of Apc^{A716} mice and $Apc^{A716} Tgfb2^{AIEC}$ mice were examined at 15 weeks of age (n=4).

For the dextran sodium sulfate (DSS) treatment experiments, $Tgfb2^{flox/flox}$ villin-CreER mice were treated with Tmx at 4 mg/mouse for three consecutive days to generate $Tgfb2^{AIEC}$ mice, and mice were treated with 2% DSS in drinking water (MP Biomedicals, Cambridge, UK) for five days. After DSS treatment, $Tgfb2^{AIEC}$ mice were treated with Tmx for two days, and were examined at three days, four weeks, six to ten weeks (n=10 for each) or 40 weeks (n=2) post-DSS treatment.

For the X-ray irradiation experiments, C57BL/6 mice and $Tgfb2^{AIEC}$ mice were irradiated with X-ray at 9 Gy (n=15 for each), and were examined for the intestine phenotype chronologically from days 0 to 6.

For azoxymethane (AOM)/DSS colitis-associated colon tumor model, wild-type mice

(n=10) were intraperitoneally injected with 10 mg/kg AOM (Sigma, St. Louis, MO), followed by treatment with 2.0% DSS (MP Biomedicals, Cambridge, UK) in drinking water for five days (week 1). This cycle was repeated twice during weeks 4 and 7, and mice were euthanized at week 15. Tumor tissues were used for immunoblotting analysis and gelatin zymography.

Histology and immunohistochemistry

The tissue sections were stained with H&E or Masson's trichrome stain, or were processed for immunohistochemistry. Staining signals of immunohistochemistry were visualized using the Vectastain Elite Kit (Vector Laboratories, Burlingame, CA). Antibodies against E-cadherin (R&D, Minneapolis, MN), α -SMA (Sigma, St. Louis, MO), F4/80 (Serotec, Oxford, UK), MT1-MMP (Gene Tex, Irvine, CA), Ki67 (Life technologies, Grand Island, NY), GFP (Molecular Probes, Eugene, OR), Collagen type IV (Nichirei Biosciences, Tokyo, Japan), CD44 (Millipore, Billerica, MA), SOX7 (R&D, Minneapolis, MN), phosphorylated Smad2 (P-Smad2) at Ser465/467 (Millipore, Billerica, MA) and β -catenin (Sigma, St Louis, MO) were used for immunohistochemistry. For fluorescence immunohistochemistry, Alexa Fluor 594 or Alexa Fluor 488 antibodies (Molecular Probes, Eugene, OR) were used as the secondary antibody. Approval for the project using human tissue sections was obtained from the Tokyo Medical and Dental University Hospital Ethics Committee.

Bone marrow transplantation

Bone marrow (BM) cells were prepared from the femurs and tibias of green fluorescent protein (GFP) gene transgenic mice. Recipient mice were irradiated with 9 Gy of X-rays, followed by intravenous injection of 2×10^6 BM cells.

Real-time reverse transcription-polymerase chain reaction (RT-PCR)

Size-classified intestinal polyps and normal intestines of *Apc*^{A716} mice (n=5 for each) were used for RNA extraction. For DSS-treated mouse samples, normal colon tissues or invasive colon tumors at three days, four weeks or six to ten weeks (n=10 for each) post-DSS treatment were used for RNA extraction. The total RNAs were reverse-transcribed using the PrimeScript RT reagent kit (Takara, Tokyo, Japan) and were PCR-amplified using SYBR Premix ExTaqII (Takara, Tokyo, Japan). The primers used for the real-time RT-PCR were purchased from Takara.

Immunoblotting analysis

Tissues were homogenized in lysis buffer, and protein sample was separated in a 10% SDS-polyacrylamide gel. Antibodies against active form of β -catenin (dephosphorylated at Ser37 and Thr41) (Millipore, Billerica, MA) and total β -catenin (Sigma, St. Louis, MO), Stat3 (Cell Signaling, Danvers, MA) and phosphorylated Stat3 at Tyr705 (Cell Signaling, Danvers, MA) were used. An anti- β -actin antibody (Sigma, St Louis, MO) was used as the internal control. The ECL detection system (GE Healthcare, Buckinghamshire, UK) was used to detect the signals.

Gelatin zymography

Tissue sample was lysed in SDS sample buffer, incubated for 20 min at 37°C and separated in a 10% polyacrylamide gel containing 0.005% gelatin labeled with Alexa Fluor 670 (Abcam, Cambridge, UK). After electrophoresis, gels were soaked in 2.5% Triton X-100 for 1 h, then gelatinolysis was carried out by incubation at 37°C for 24 h. The gel was monitored by an Odyssey™ infrared imaging system (LI-COR, Lincoln, NE).

Organoid culture

The organoid culture using small intestinal epithelial cells was performed as described previously (18). Briefly, organoids were cultured in Matrigel with Advanced DMEM/F12 medium (Invitrogen, Carlsbad, CA) supplemented with 50 ng/ml EGF (Invitrogen, Carlsbad, CA), R-Spondin1 conditioned medium (a kind gift from Dr. Marc Leushacke) and 100 ng/ml Noggin (Peprotech, Rocky Hill, NJ). The cultures were passaged once, and the crypt length was measured under a dissecting microscope.

Organoid cell proliferation was detected using the Click-iT EdU Imaging System (Invitrogen, Carlsbad, CA). After EdU staining, organoids were incubated with anti-CD44 antibody (Chemicon, Temecula, CA) followed by secondary antibody, Alexa Fluor 488 (Molecular Probes, Eugene, OR). The stained organoids were analyzed using a Zeiss 510 META laser-scanning microscope (Zeiss, Thornwood, NY).

Statistical analyses

The data were analyzed using an unpaired *t*-test, and are presented as the means \pm standard deviation (s.d.). A value of $P < 0.05$ was considered as statistically significant.

Results

Size-dependent submucosal invasion of intestinal tumors

It has been demonstrated that the disruption of *Tgfb2*, *Smad4* or *Smad3* in *Apc* mutant mice causes development of invasive adenocarcinomas in the intestine, whereas simple *Apc* mutant mice develop only benign adenomas (12, 19-21). Accordingly, the combination of Wnt signaling activation and TGF β signaling suppression is implicated in the malignant invasion of intestinal tumors. To further investigate the mechanism underlying the submucosal invasion of intestinal tumors, we constructed compound mutant mice carrying both *Apc*^{A716} and *Tgfb2* mutation in intestinal epithelial cells (*Apc*^{A716}*Tgfb2* ^{Δ IEC}). We confirmed that *Apc*^{A716} *Tgfb2* ^{Δ IEC} mice developed adenocarcinomas with submucosal invasion, whereas simple *Apc*^{A716} mice had only non-invasive adenomas (Fig. 1A and Supplementary Fig. S1). Notably, only the polyps > 1 mm in diameter showed submucosal invasion in the *Apc*^{A716} *Tgfb2* ^{Δ IEC} mice (Fig. 1B and Supplementary Fig. S1B). Histologically, large invasive polyps in *Apc*^{A716} *Tgfb2* ^{Δ IEC} mice were associated with increased stroma and macrophage infiltration, which was not found in the small non-invasive polyps (Fig. 1C). Metalloproteinase-1 (MT1-MP) expression was induced in the stroma of the large invasive tumors, and collagen fiber deposition was also found in the stroma by Masson's trichrome staining. Moreover, expression of IL-1 β , IL-6 and COX-2 was induced when polyp size increased beyond > 1 mm in diameter in *Apc*^{A716} mouse small intestine, and expression levels of MT1-MMP, Adam10 and epiregulin were also increased in the large polyps (Fig. 1D). The induction of these factors was also found in the colon polyps > 2 mm in diameter. By a laser microdissection-based RT-PCR analysis, we found that these factors, except for Adam10,

were predominantly expressed in the tumor stroma (Supplementary Fig. S2). Taken together, these results indicate that the inflammatory microenvironment is generated by a tumor size-dependent mechanism in both the small intestinal and colon polyps. It is therefore possible that such microenvironment is required for submucosal invasion.

Submucosal invasion by TGF β signaling suppression and ulcerative colitis

We thus examined the role of inflammatory responses in TGF β signaling suppression-associated submucosal invasion using a colitis mouse model by treating *Tgfb2*^{ΔIEC} mice with DSS (Fig. 2A). The wild-type mice treated with DSS showed ulcerative colitis beginning three days after DSS treatment, and the colonic mucosa was repaired in four weeks post-treatment (Fig. 2B). Although mucosal ulcers were repaired in the *Tgfb2*^{ΔIEC} mice in four weeks post-DSS treatment, regeneration of the normal gland structure was significantly impaired (Fig. 2B, asterisk). Importantly, colonic epithelial cells invaded to the submucosa in *Tgfb2*^{ΔIEC} mice by the end of fourth week post-treatment. These invading epithelial cells continued proliferation, and formed invasive tumors associated with deposition of collagen fibers by the 10 weeks post DSS treatment (Fig. 2C). Furthermore, large solid tumors were visible from outside of the colon and cecum of *Tgfb2*^{ΔIEC} mice by the 40th week post-treatment (Fig. 2D). Epithelial cells of tumors were positive for Ki67, indicating that the tumor cells continued proliferation even at 40 weeks post-DSS treatment. We confirmed that disruption of *Tgfb2* in normal intestinal mucosa did not cause any morphological changes (Supplementary Fig. S3), which is consistent with previous reports (20, 22). The level of active β -catenin was significantly increased both in the *Apc*^{Δ716} mouse intestinal tumors and

colitis-associated colon tumors that were chemically induced by treatment with AOM and DSS, however, active β -catenin level was not increased in the invasive tumors of DSS-treated *Tgfr2^{ΔIEC}* mice (Fig. 2E). These results indicate that ulcerative colitis induces invasive tumors in the TGF β -suppressed mucosa without activation of the Wnt signaling.

We next examined human inflammatory bowel disease (IBD)-related colon cancer. Nuclear localized P-Smad2 was found in the surface epithelial cells of ulcerative colitis (UC), however, it was not detected in the invaded tumor cells, indicating that there was suppression of TGF β signaling (Fig. 2F). A loss of P-Smad2 staining in tumor cells was found in five out of eight cases (62.5%) of UC-associated colon cancer. Moreover, β -catenin accumulation was not detected in seven out of eight UC-associated tumors (87.5%). Accordingly, it is possible that suppression of TGF β signaling causes colon cancer invasion in human IBD patients without Wnt signaling activation.

Chronic inflammatory responses in the invasive tumors

We found that bone marrow-derived cells and macrophages infiltrated in the stroma of invasive colon tumors, but not in the non-invasive mucosa of DSS-treated *Tgfr2^{ΔIEC}* mice (Fig. 3A). Consistently, expression of monocyte-trophic chemokines (23), CCL2, CCL3, CCL4, CCL7 and CCL8, was increased significantly in the invasive colon tumors (Fig. 3B). Moreover, Stat3 was constitutively phosphorylated in the invasive tumors of DSS-treated *Tgfr2^{ΔIEC}* mice, whereas its level was decreased in the repaired mucosa of DSS-treated wild-type mice (Fig. 3C). These results indicate that inflammatory responses are chronically maintained in the invasive tumor tissues, even after the repair of DSS-induced ulcers.

We thus determined the levels of inflammatory cytokines in both the invasive tumors and DSS-induced ulcerative colitis. Expression was significantly upregulated for TNF- α , IL-1 β , IL-6, CXCL1, CXCL2 and COX-2 by DSS-induced ulcerative colitis in both the wild-type and *Tgfb β 2^{ΔIEC}* mice (Fig. 3D, yellow and blue circles, respectively), whereas the levels of these factors in wild-type mice decreased significantly after the mucosa was repaired (Fig. 3D, green circles). In the invasive tumors of the *Tgfb β 2^{ΔIEC}* mice, expression of TNF- α , IL-6 and CXCL2 remained high, whereas that of IL-1 β , CXCL1 and COX-2 decreased to the level of repaired mucosa (Fig. 3D, red circles). These results indicate that different types of inflammatory responses are induced in the invasive tumor tissues of the *Tgfb β 2^{ΔIEC}* mice compared with those in the mice with DSS-induced acute colitis.

Expression of MT1-MMP and activation of MMP2 in invasive tumors

To investigate the mechanism underlying chronic inflammation-associated invasion, we examined expression of MMPs that are important for submucosal invasion (24). It has been shown that MT1-MMP plays a key role in activation of MMP2 (25) and MT1-MMP is expressed in macrophages, regulating inflammatory responses (26, 27). The expression levels of MT1-MMP, MMP2 and MMP9 were significantly increased in the invasive tumors of DSS-treated *Tgfb β 2^{ΔIEC}* mice (Fig. 4A). Fluorescence immunohistochemistry showed that the stromal cells of invasive tumors expressed MT1-MMP, and most MT1-MMP-expressing cells in tumor stroma were F4/80-positive macrophages (Fig. 4B). Moreover, gelatin zymography analyses revealed that MMP2 was activated in the invasive tumor tissues, but not in the normal colonic mucosa of the same DSS-treated *Tgfb β 2^{ΔIEC}* mice (Fig. 4C).

Consistently, the immunostaining signal for collagen type IV in the basement membrane was significantly decreased in the invading epithelial cells (Fig. 4D). These results suggest that chronic inflammation contributes to the submucosal invasion through macrophage-expressed MT1-MMP, which leads to MMP2 activation resulting in degradation of basement membrane.

Because MT1-MMP expression was also induced in the *Apc*^{A716} benign adenomas (Fig. 1C, D), we further examined MMP activation in other mouse tumor models. As anticipated, MMP2 was activated in the invasive tumors of *Apc*^{A716} *Tgfb2*^{ΔIEC} mice (Fig. 4E). Notably, MMP2 activation was also found in the non-invasive benign tumors of *Apc*^{A716} mice and AOM/DSS-treated mice, although the band intensities were lower compared with those of the *Apc*^{A716} *Tgfb2*^{ΔIEC} mouse invasive tumors (Fig. 4E). These results suggest that MMP2 activation is already induced in benign intestinal tumors, and its activation level increases with the progression of the tumor. Accordingly, it is also possible that suppression of TGFβ signaling causes acquisition of invasiveness of epithelial cells in such microenvironment.

Impaired mucosal regeneration by suppression of TGFβ signaling

Impaired mucosal regeneration from ulcer in *Tgfb2*^{ΔIEC} mice (Fig. 2B, C) suggested a role of TGFβ signaling in regeneration of injured intestinal mucosa. To test this possibility, mice were irradiated with X-ray at 9 Gy. In the irradiated wild-type mice, the number of proliferating cells in the crypt decreased on days 1-3 after irradiation, followed by destruction of the mucosal structure by day 4 (Supplementary Fig. S4). At the same time, the undifferentiated cell population expanded, and normal crypt-villous structures were regenerated by day 6, which was consistent with a previous report (28). X-ray irradiation in

Tgfb β 2^{ΔIEC} mice also showed a decrease in the proliferating crypt cell population, followed by increased numbers of proliferating undifferentiated cells (Supplementary Fig. S4). However, the extent of the injury was more severe in the *Tgfb β 2^{ΔIEC}* mice, and the regeneration of the normal mucosal structure was impaired in both the small intestine and colon (Fig. 5A and Supplementary Fig. S5). Because of such severe phenotypes, most irradiated *Tgfb β 2^{ΔIEC}* mice died by day 7 (Fig. 5B). Moreover, markers of undifferentiated epithelial cells, CD44 and SOX7, were expressed in the entire intestinal mucosa of the X-ray-irradiated *Tgfb β 2^{ΔIEC}* mice, whereas their expression was limited to the crypt bottom in the wild-type mice (Fig. 5A and Supplementary Fig. S5B). Consistently, an intestinal progenitor cell marker, SOX9 (29), was upregulated in the intestine by irradiation, and the SOX9 level was significantly higher in *Tgfb β 2^{ΔIEC}* mice than in wild-type mice (Fig. 5C). Moreover, the nuclear accumulation and stabilization of β -catenin was not found in the irradiated *Tgfb β 2^{ΔIEC}* mouse intestinal epithelia (Figs. 5D and E). Taken together, these results indicate that TGF β signaling is required for differentiation of regenerating epithelial cells, and that blocking TGF β pathway causes expansion of the proliferating and undifferentiated epithelial cell population without activation of Wnt signaling.

Acquisition of invasive phenotype by blocking TGF β signaling in regenerating epithelial cells

We next studied the effect of TGF β signaling suppression in regenerating mucosa on invasive phenotype. Organoid culture of the irradiated wild-type mouse-derived intestinal epithelial cells showed budding from cysts, forming mini-crypt structures (Fig. 6A), which was

consistent with the original report (18). Importantly, intestinal epithelial cells derived from irradiated *Tgfb β 2^{ΔIEC}* mice formed gland-like long crypt structures in the Matrigel (Fig. 6A). We further examined the epithelial cell proliferation in the organoids by evaluating the EdU incorporation to nuclei, and examined the undifferentiated status by determining the CD44 expression. Notably, the expression of EdU and CD44 was found in the epithelial cells along the long crypts of *Tgfb β 2^{ΔIEC}* mouse-derived organoids, although that was detected only in budding crypts of wild-type organoids. These results suggest that the long crypts are comprised of proliferating undifferentiated epithelial cells. The proportion of long crypts > 200 μm was significantly higher in the irradiated *Tgfb β 2^{ΔIEC}* mouse-derived intestinal epithelial cells ($42 \pm 13\%$ of all crypts) compared with epithelial cells derived from irradiated *Tgfb β 2^{flox/flox}* control mice ($3.9 \pm 4.5\%$) (Fig. 6B). Such long crypt formation was not found also in organoids of non-irradiated *Tgfb β 2^{ΔIEC}* mouse-derived intestinal epithelial cells. It is possible that long crypt formation in Matrigel reflects “collective cell migration” in the extracellular matrix, which is one of strategies used by cancer cells for invasion (30). Therefore, it is conceivable that suppression of TGFβ signaling in regenerating mucosa results in the acquisition of invasive phenotype, which leads to collective migration in the inflammatory microenvironment.

Discussion

Genome-wide analyses have indicated that accumulation of genetic alterations in oncogenic and tumor suppressor pathways is responsible for development of colon cancer (31). On the other hand, the nature and significance of the individual genetic alterations are not yet understood (32). In addition, relatively few mutations have been identified that are responsible for invasion and/or metastasis (8, 33), suggesting that microenvironment can promote malignant progression. We have herein demonstrated that simple genetic alterations in the TGF β pathway can lead to the development of invasive gastrointestinal cancers without additional genetic alterations when the mucosa is inflamed and regenerating from injury (Fig. 7A).

It has been shown that suppression of TGF β signaling in the intestinal and mammary gland tumor cells induces chemokine expression, which recruits myeloid cells to the tumor microenvironment (12, 14). These myeloid cells express metalloproteinases, such as MT1-MMP, MMP2 and MMP9 that contribute to the invasion or metastasis of tumor cells. These results suggest that elaboration of an inflammatory microenvironment is critical for the malignant progression mediated by inhibition of the TGF β signaling. We also found that MMP2 is activated by macrophage-expressing MT1-MMP in the invasive tumors. However, we found that MMP2 is activated also in the benign intestinal tumor tissues with intact TGF β signaling. Accordingly it is conceivable that the acquisition of an invasive phenotype by epithelial cells is further required for malignant progression where TGF β signaling is suppressed.

Blocking TGF β signaling in the intestinal epithelial cells did not cause morphological

changes, indicating that TGF β signaling is not required for differentiation of normal intestinal stem/progenitor cells (20, 22). However, we found that suppression of TGF β signaling in the injured intestinal mucosa blocked mucosal regeneration by suppressing differentiation, which caused the expansion of undifferentiated cell population. Accordingly, TGF β signaling is essential for regeneration from damaged mucosa in the gastrointestinal tract. Notably, intestinal epithelial cells derived from irradiated *Tgfb2*^{ΔIEC} mice showed increased invasion in Matrigel, possibly caused by expansion of undifferentiated epithelial cell population. However, irradiation of *Tgfb2*^{ΔIEC} mice caused only dysplastic changes without tumor development, indicating that blocking TGF β signaling in regenerating epithelial cells alone is insufficient for induction of invasive tumors.

Accordingly, it is required for the development of invasive tumors that both the inflammatory microenvironment where MT1-MMP is expressed and the regenerating epithelial cells with increased invasiveness by inhibition of TGF β signaling (Fig. 7A). Such a mechanism is possibly important for cancer development associated with IBD. In IBD lesions, the mucosa is continuously regenerating in a chronic inflammatory microenvironment, and the expression of MT1-MMP, together with inflammatory chemokines, is upregulated similar to that observed in *Tgfb2*^{ΔIEC} mouse tumors (Supplementary Fig. S6). Furthermore, we herein demonstrated that TGF β signaling is suppressed and Wnt signaling is not activated in more than 60% of UC-related colon cancer cells. Consistently, it has also been reported that human colitis-associated colon cancer does not follow the adenoma-carcinoma sequence, and mutations in β -catenin or APC are not common either (34). Accordingly, simple genetic alterations in the TGF β signaling pathway may cause the development of invasive tumors

under IBD condition (Fig. 7A).

On the other hand, compound mutant mice carrying mutations in *Apc* and TGF β pathway genes showed progression of invasive adenocarcinomas from Wnt activated adenomas (19-21), indicating that the combination of Wnt activation and TGF β signaling suppression is sufficient for malignant progression. In the regenerating mucosa, stem cell population is expanded, with the signaling in the Wnt and Notch pathways activated (35). It is therefore possible that the activation of Wnt signaling is necessary for malignant progression in sporadic tumors where TGF β signaling is blocked without mucosa regeneration. Accordingly, combination of Wnt activation and TGF β suppression in the MT1-MMP-expressing inflammatory microenvironment is sufficient for the induction of invasive adenocarcinoma in normal intestine (Fig. 7B).

In conclusion, we have demonstrated that suppression of TGF β signaling in the regenerating epithelial cells results in suppression of epithelial differentiation and acquisition of invasive phenotype of epithelial cells. Chronic inflammation induces development of an MMP2-activating microenvironment. The cooperation between TGF β signaling suppression in the regenerating epithelia and the inflammatory microenvironment can cause invasive colon cancer development, which may explain mechanism of IBD-associated colon tumorigenesis. Therefore, controlling the inflammatory microenvironment may help an effective preventive or therapeutic strategy against the malignant progression of colon cancer.

Acknowledgements

The authors thank Manami Watanabe and Ayako Tsuda for technical assistance.

References

1. Coussens LM, Werb Z. Inflammation and cancer. *Nature* 2002;420:860-7.
2. Elinav E, Nowarski R, Thaïss CA, Hu B, Jin C, Flavell RA. Inflammation-induced cancer: crosstalk between tumours, immune cells and microorganisms. *Nat Rev Cancer* 2013;13:759-71.
3. Oshima M, Dinchuk JE, Kargman SL, Oshima H, Hancock B, Kwong E, et al. Suppression of intestinal polyposis in *Apc^{A716}* knockout mice by inhibition of cyclooxygenase 2 (COX-2). *Cell* 1996;87:803-9.
4. Sonoshita M, Takaku K, Sasaki N, Sugimoto Y, Ushikubi F, Narumiya S, et al. Acceleration of intestinal polyposis through prostaglandin receptor EP2 in *Apc^{A716}* knockout mice. *Nat Med* 2001;7:1048-51.
5. Greten FR, Eckmann L, Greten TF, Park JM, Li ZW, Egan LJ, et al. IKK β links inflammation and tumorigenesis in a mouse model of colitis-associated cancer. *Cell* 2004;118:285-96.
6. Bollrath J, Phesse TJ, von Burstin VA, Putoczki T, Bennecke M, Batemen T, et al. gp130-mediated Stat3 activation in enterocytes regulates cell survival and cell-cycle progression during colitis-associated tumorigenesis. *Cancer Cell* 2009;15:91-102.
7. Grivennikov S, Karin E, Terzic J, Mucida D, Yu GY, Vallabhapurap, S, et al. IL-6 and Stat3 are required for survival of intestinal epithelial cells and development of colitis-associated cancer. *Cancer Cell* 2009;15:103-13.
8. Markowitz SD, Bertagnolli MM. Molecular basis of colorectal cancer. *N Eng J Med* 2009;361:2449-60.
9. Trobridge P, Knoblaugh S, Washington MK, Munoz NM, Tsuchiya KD, Rojas A, et al. TGF- β

- receptor inactivation and mutant *Kras* induce intestinal neoplasms in mice via a β -catenin-independent pathway. *Gastroenterology* 2009;136:1680-8.
10. Yu M, Trobridge P, Wang Y, Kanngum S, Morris SM, Knoblaugh S, et al. Inactivation of TGF β signaling and loss of *PTEN* cooperate to induce colon cancer *in vivo*. *Oncogene* 2013;33:1538-47.
 11. Ikushima H, Miyazono K. TGF β signaling: a complex web in cancer progression. *Nat Rev Cancer* 2010;10:415-24.
 12. Kitamura T, Kometani K, Hashida H, Matsunaga A, Miyoshi H, Hosogi H, et al. SMAD4-deficient intestinal tumors recruit CCR1+ myeloid cells that promote invasion. *Nat Genet* 2007;39:467-75.
 13. Kitamura T, Fujishita T, Loetscher P, Revesz L, Hashida H, Kizaka-Kondoh S, et al. Inactivation of chemokine (C-C motif) receptor 1 (CCR1) suppresses colon cancer liver metastasis by blocking accumulation of immature myeloid cells in a mouse model. *Proc Natl Acad Sci, USA*. 2010;107:13063-8.
 14. Yang L, Huang J, Ren X, Gorska AE, Chytil A, Aakre M, et al. Abrogation of TGF β signaling in mammary carcinomas recruits Gr-1+CD11b+ myeloid cells that promote metastasis. *Cancer Cell* 2008;13:23-35.
 15. Oshima M, Oshima H, Kitagawa K, Kobayashi M, Itakura C, Taketo M. Loss of *Apc* heterozygosity and abnormal tissue building in nascent intestinal polyps in mice carrying a truncated *Apc* gene. *Proc Natl Acad Sci USA* 1995;92:4482-6.
 16. Chytil, A, Magnuson MA, Wright CVE, Moses HL. Conditional inactivation of the TGF- β type II receptor using Cre;Lox. *Genesis* 2002;32:73-5.

17. el Marjou F, Janssen KP, Chang BH, Li M, Hindie V, Chan L, et al. Tissue-specific and inducible Cre-mediated recombination in the gut epithelium. *Genesis* 2004;39:186-93.
18. Sato T, Vries RG, Snippert HJ, van de Wetering M, Barker N, Stange DE, et al. Single Lgr5 stem cells build crypt-villus structures *in vitro* without a mesenchymal niche. *Nature* 2009;459:262-6.
19. Takaku K, Oshima M, Miyoshi H, Matsui M, Seldin MF, Taketo MM. Intestinal tumorigenesis in compound mutant mice of both Dpc4 (Smad4) and Apc genes. *Cell* 1998;92:645-56.
20. Munoz, NM, Upton M, Rojas A, Washington MK, Lin L, Chytil A, et al. Transforming growth factor β receptor type II inactivation induces the malignant transformation of intestinal neoplasms initiated by Apc mutation. *Cancer Res.* 2006;66:9837-44.
21. Sodir NM, Chen X, Park R, Nickel AE, Conti PS, Moats R, et al. Smad3 deficiency promotes tumorigenesis in the distal colon of *Apc^{Min/+}* mice. *Cancer Res.* 2006;66:8430-8.
22. Biswas S, Chytil A, Washington K, Romero-Gallo J, Gorska AE, Wirth PS, et al. Transforming growth factor β receptor type II inactivation promotes the establishment and progression of colon cancer. *Cancer Res.* 2004;64:4687-92.
23. Mantovani A, Bonecchi R, Locati M. Tuning inflammation and immunity by chemokine sequestration: decoys and more. *Nat Rev Immunol* 2006;6:907-18.
24. Egeblad M, Werb Z. New functions for the matrix metalloproteinase in cancer progression. *Nat Rev Cancer* 2002;2:161-74.
25. Sato H, Takino T. Coordinate action of membrane-type matrix metalloproteinase-1 (MT1-MMP) and MMP-2 enhances pericellular proteolysis and invasion. *Cancer Sci.* 2010;101:843-7.

26. Koziol A, Martin-Alonso M, Clemente C, Gonzalo P, Arroyo AG. Site-specific cellular functions of MT1-MMP. *Eur J Cell Biol* 2012;91:889-95.
27. Akla N, Pratt J, Annabi B. Concanavalin-A triggers inflammatory response through JAK/STAT3 signalling and modulates MT1-MMP regulation of COX-2 in mesenchymal stromal cells. *Exp Cell Res* 2012;318:2498-506.
28. van Landeghem L, Santoro MA, Krebs AE, Mah AT, Dehmer JJ, Gracz AD, et al. Activation of two distinct Sox9-EGFP-expressing intestinal stem cell populations during crypt regeneration after irradiation. *Am J Gastrointest Liver Physiol* 2012;302:G1111-32.
29. Furuyama K, Kawaguchi Y, Akiyama H, Horiguchi M, Kodama S, Kuhara T, et al. Continuous cell supply from a Sox9-expressing progenitor zone in adult liver, exocrine pancreas and intestine. *Nat Genet* 2011;43:34-41.
30. Friedl P, Wolf K. Tumour-cell invasion and migration: diversity and escape mechanisms. *Nat Rev Cancer* 2003;3:362-74.
31. The Cancer Genome Atlas Network. Comprehensive molecular characterization of human colon and rectal cancer. *Nature* 2012;487:330-6.
32. Fearon E. Molecular genetics of colorectal cancer. *Annu Rev Pathol* 2011;6:479-507.
33. Vogelstein B, Papadopoulos NP, Velculescu VE, et al. Cancer genome landscapes. *Science* 2013;339:1546-1558.
34. Rogler G. Chronic ulcerative colitis and colorectal cancer. *Cancer Lett* 2014;345:235-41.
35. Tan S, Barker N. Epithelial stem cells and intestinal cancer. *Semin Cancer Biol* 2014 *in press*.

Figure Legends

Figure 1. Size-dependent submucosal invasion of intestinal tumors. (A) Representative photographs of *Apc*^{A716} mouse benign adenomas (*left*) and *Apc*^{A716} *Tgfbr2*^{ΔIEC} mouse invasive adenocarcinomas (*right*). H&E (*top*) and enlarged images of the boxed areas (*middle*), and fluorescence immunohistochemistry for E-cadherin (*red*) and αSMA (*green*) (*bottom*). T, tumor; and SM, submucosa. Arrowheads indicate submucosal invasion of tumor epithelial cells. Bars, 400 μm (*top*) and 200 μm (*middle* and *bottom*). (B) Size classification of intestinal tumors of *Apc*^{A716} mice (*top*) and *Apc*^{A716} *Tgfbr2*^{ΔIEC} mice (*bottom*) scored using “Swiss roll” histology sections. Each dot indicates an individual polyp. Different colors indicate independent mice. (C) Representative photographs of non-invasive (*top*) and invasive polyps (*bottom*) of *Apc*^{A716} *Tgfbr2*^{ΔIEC} mice. H&E staining, immunohistochemistry for F4/80 and MT1-MMP, and Masson’s trichrome staining (MT) (*left to right*). Insets indicate high-powered magnification. Bars, 200 μm (*top*) and 400 μm (*bottom*). (D) Expression levels of the indicated factors relative to the mean level of normal mucosa in size-classified small intestinal and colon tumors of *Apc*^{A716} mice (mean ± s.d.). Asterisks, *P* < 0.05 compared with the normal mucosal level.

Figure 2. Submucosal invasion of TGFβ signaling-suppressed cells by ulcerative colitis. (A) Schedule for Tmx and DSS treatment and examination of mice. (B) Representative photographs (H&E) of DSS-treated wild-type (*left*) and DSS-treated *Tgfbr2*^{ΔIEC} (*right*) mouse colons three days (*top*) and four weeks (*down*) post-treatment. Arrows (*top*) indicate ulcer lesions. Arrowheads (*bottom right*) indicate submucosal invasion of epithelial cells.

Asterisk indicates impaired regeneration of the normal gland structure. Bars, 200 μm . (C) Representative photographs of serial sections of invasive tumors of a DSS-treated *Tgfr2^{ΔIEC}* mouse 10 weeks post-treatment. H&E (*top*), Masson's trichrome (MT) staining (*middle*) and enlarged images of the boxed areas (*bottom*). Arrows indicate the location of muscularis mucosae. Asterisks indicate impaired regeneration of the normal gland structure. Bars, 500 μm (*top* and *middle*) and 200 μm (*bottom*). (D) Representative macroscopic photographs of invasive tumors developed in a DSS-treated *Tgfr2^{ΔIEC}* mouse at 40 weeks post-treatment (arrows, *top left*), and the H&E (*top right*) and immunohistochemistry for Ki67 (*bottom*). Arrows (*bottom*) indicate the location of muscularis mucosae, and inset indicates an enlarged image of the boxed area. Ce, cecum; Ile, ileum and Co, colon. Bars, 2 mm (*top*) and 400 μm (*bottom*). (E) Immunoblotting for active β -catenin and total β -catenin in the intestinal mucosa and polyps in *Apc^{A716}* and AOM/DSS-treated mice (*left*) and DSS-treated *Tgfr2^{ΔIEC}* mice (*right*) at the indicated time points. NM, normal mucosa; and inv, invasive tumors. β -Actin was used as an internal control. (F) Representative immunohistochemical findings of p-Smad2 in UC-associated human colon cancer tissues (*left, center*), and the β -catenin in sporadic colon cancer (*right top*) and UC-associated colon cancer (UC) (*right bottom*). Arrows (*center*) indicate surface epithelial cells and invading tumor cells. Bars, 500 μm (*left*) and 50 μm (*center* and *right*).

Figure 3. Chronic inflammation in invasive tumors of *Tgfr2^{ΔIEC}* mice. (A) Representative photographs of immunohistochemistry for GFP in a DSS-treated *Tgfr2^{ΔIEC}* mouse that had undergone bone marrow transplantation from a GFP transgenic mouse (*top*). Enlarged

images of invasive (*bottom left*) and non-invasive (*bottom center*) mucosa of the boxed areas (*top*). Fluorescent immunostaining for F4/80 (*green*) and E-cadherin (*red*) in an invasive tumor (*bottom right*). Bars, 400 μm (*top*) and 200 μm (*bottom*). (B) Relative expression levels of the indicated chemokines in the invasive tumors in DSS-treated *Tgfb2^{ΔIEC}* mice to the mean level of wild-type mouse colons (mean \pm s.d.). Asterisks, $P < 0.05$. (C) Immunoblotting for phosphorylated Stat3 and total Stat3 in the colon mucosa of control wild-type mice (*WT*), DSS-treated wild-type and *Tgfb2^{ΔIEC}* mice. β -Actin was used as an internal control. uc, ulcerative colitis; rep, repaired mucosa; and inv, invasive tumor. The band intensities for pStat3/Stat3 relative to the mean level of wild-type mice (*WT*) (red bar) are shown in a bar graph (*C, bottom*). (D) Expression levels of cytokines, chemokines and COX-2 in DSS-treated wild-type or *Tgfb2^{ΔIEC}* mouse colonic mucosa relative to the mean levels of the repaired mucosa (*green*) (mean \pm s.d.). Asterisks, $P < 0.05$. ns, not significant.

Figure 4. Expression of MT1-MMP and activation of MMP2 in invasive tumors. (A) Expression levels of indicated MMPs in the DSS-treated *Tgfb2^{ΔIEC}* mouse invasive tumors (*red*) relative to the level of repaired mucosa of DSS-treated wild-type mice (*green*) (mean \pm s.d.). Asterisks, $P < 0.05$ versus wild-type level. (B) Fluorescent immunostaining of the invasive tumors in DSS-treated *Tgfb2^{ΔIEC}* mice for E-cadherin (*green*), MT1-MMP (*red*) (*left*), and F4/80 (*green*) and MT1-MMP (*red*) (*right*). Insets indicate enlarged images of the boxed areas. Bars, 200 μm . (C) Gelatin zymography of the normal mucosa (*N1-N3*) and invasive tumors (*T1-T3*) of three individual DSS-treated *Tgfb2^{ΔIEC}* mice. Latent MMP9 and MMP2

were used as positive controls. (D) Immunostaining for collagen type IV in the invasive colon tumors of DSS-treated *Tgfb2*^{ΔIEC} mice. White arrowheads indicate invading epithelial cells in submucosa, whereas closed arrowheads indicate non-invading epithelial cells. Bars, 50 μm. (E) Gelatin zymography of the normal intestinal mucosa (N1-N2) and intestinal adenomas (A1-A2) of *Apc*^{Δ716} mice, invasive adenocarcinomas (C1-C2) of *Apc*^{Δ716} *Tgfb2*^{ΔIEC} mice, ulcerative colitis tissues of DSS-treated wild-type mice (I1-I2), repaired mucosa of DSS-treated wild-type mice (R1-R2) and non-invasive colon tumors (T1-T2) of AOM/DSS-treated wild-type mice. Coomassie Brilliant Blue staining of the 40 kDa bands are shown at the bottom of the zymography gels as a protein level control (C, E). Relative band intensities for active MMP2 to the mean level of *Apc*^{Δ716} adenomas (red bar) are shown in a bar graph (E, bottom).

Figure 5. Impaired mucosal regeneration by suppression of TGFβ signaling. (A) Representative photographs of X-ray-irradiated wild-type (top) and *Tgfb2*^{ΔIEC} (bottom) mouse small intestines six days post-irradiation. H&E staining, fluorescence immunostaining for E-cadherin (red) and Ki67 (green), immunohistochemistry for CD44 and SOX7 (left to right) are shown. White arrowheads indicate Ki67-positive cells. Arrows and closed arrowheads indicate CD44- and SOX7-positive epithelial cells, respectively. Bars, 200 μm (left) and 100 μm (center and right). (B) Survival curve of wild-type and *Tgfb2*^{ΔIEC} mice after X-ray irradiation at 9 Gy. (C) Expression levels of SOX9 in X-ray-irradiated wild-type (gray bars) and *Tgfb2*^{ΔIEC} (closed bars) mouse intestines relative to the mean level of non-irradiated wild-type mice (Day 0) (mean ± s.d.). Asterisks, *P* < 0.05 versus Day 0 level, and the dagger

indicates $P < 0.05$. ns, not significant. (D) Immunohistochemical staining for β -catenin in an Apc^{A716} mouse intestinal polyp (*left*) and irradiated $Tgfr2^{AIEC}$ mouse small intestinal mucosa (*right*). White arrowheads indicate β -catenin nuclear accumulation. Bar, 25 μ m. (E) Immunoblotting for active β -catenin and total β -catenin in the indicated intestinal tissues. β -Actin was used as an internal control.

Figure 6. Acquisition of invasive phenotype by TGF β inhibition in regenerating epithelia. (A) Representative bright field photographs of organoid cultures in Matrigel (*left*) and confocal images of organoids immunostained for EdU (*red*) and CD44 (*green*) (*right*) of wild-type (*top*) and X-ray-irradiated $Tgfr2^{AIEC}$ (*bottom*) mouse intestinal epithelia. Arrowheads indicate EdU negative and CD44 weak cells in wild-type organoid. Bars, 200 μ m (*left*) and 50 μ m (*right*). (B) The crypt lengths of organoids derived from wild-type and non-irradiated $Tgfr2^{AIEC}$ mice (*light blue*), irradiated $Tgfr2^{flox/flox}$ (control) mice (*blue*) and irradiated $Tgfr2^{AIEC}$ mice (*red*). Red bar indicates 200 μ m threshold, and crypts longer than 200 μ m were judged to be long crypts.

Figure 7. A schematic drawing of the TGF β signaling suppression-induced invasive tumor development in regenerating and inflamed mucosa (A) and in Wnt signaling-activated adenomas (B).

Figure 1

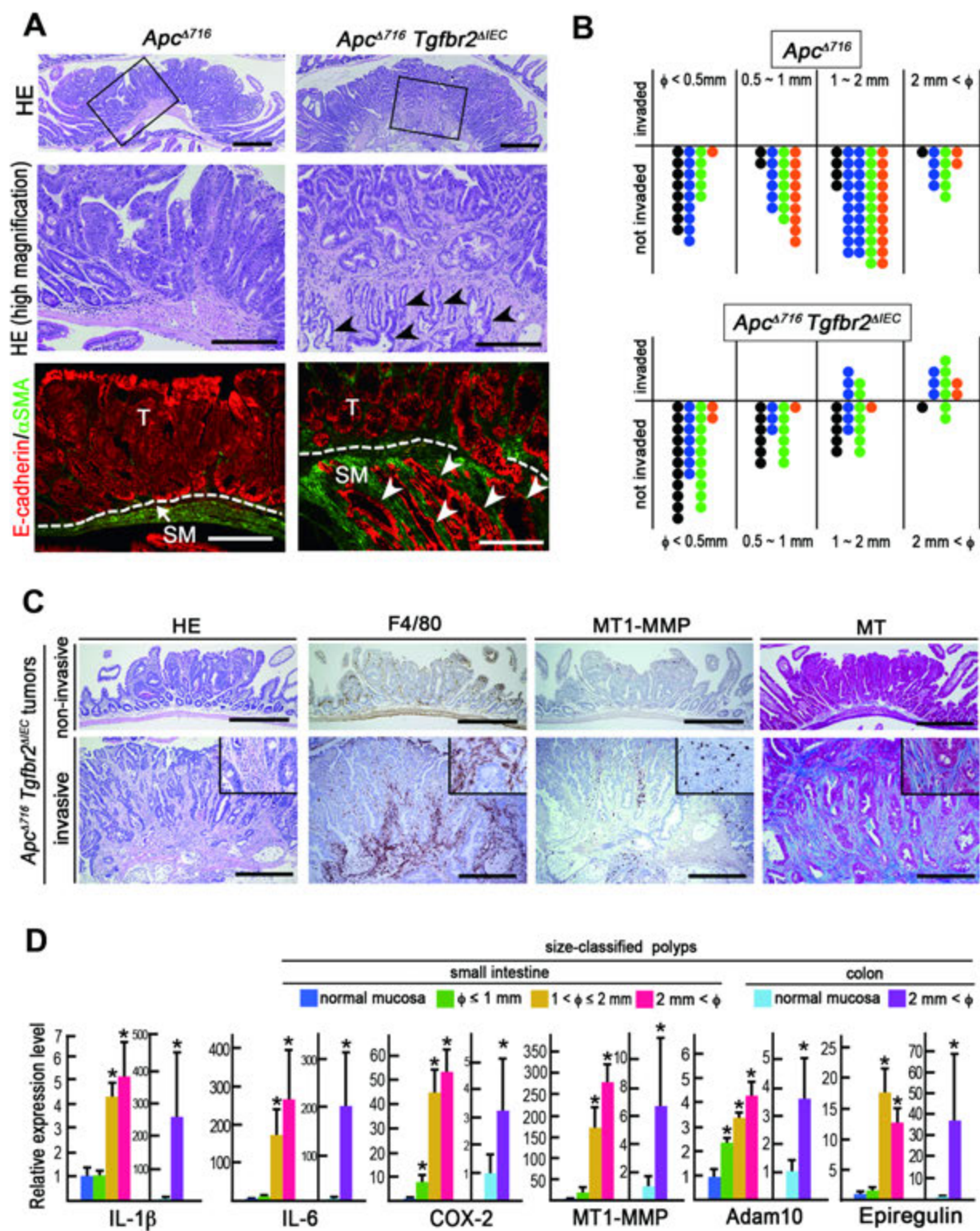


Figure 2

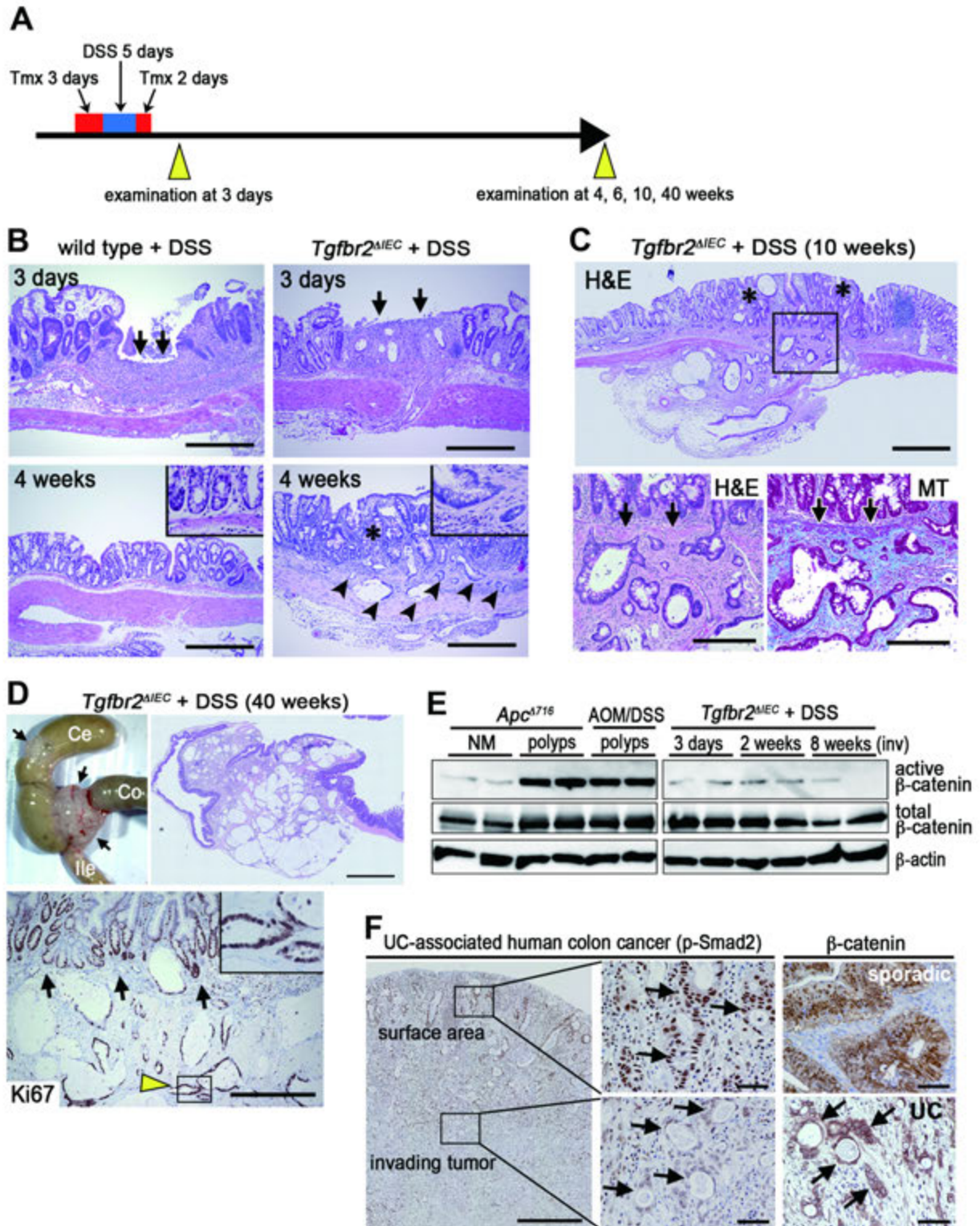


Figure 3

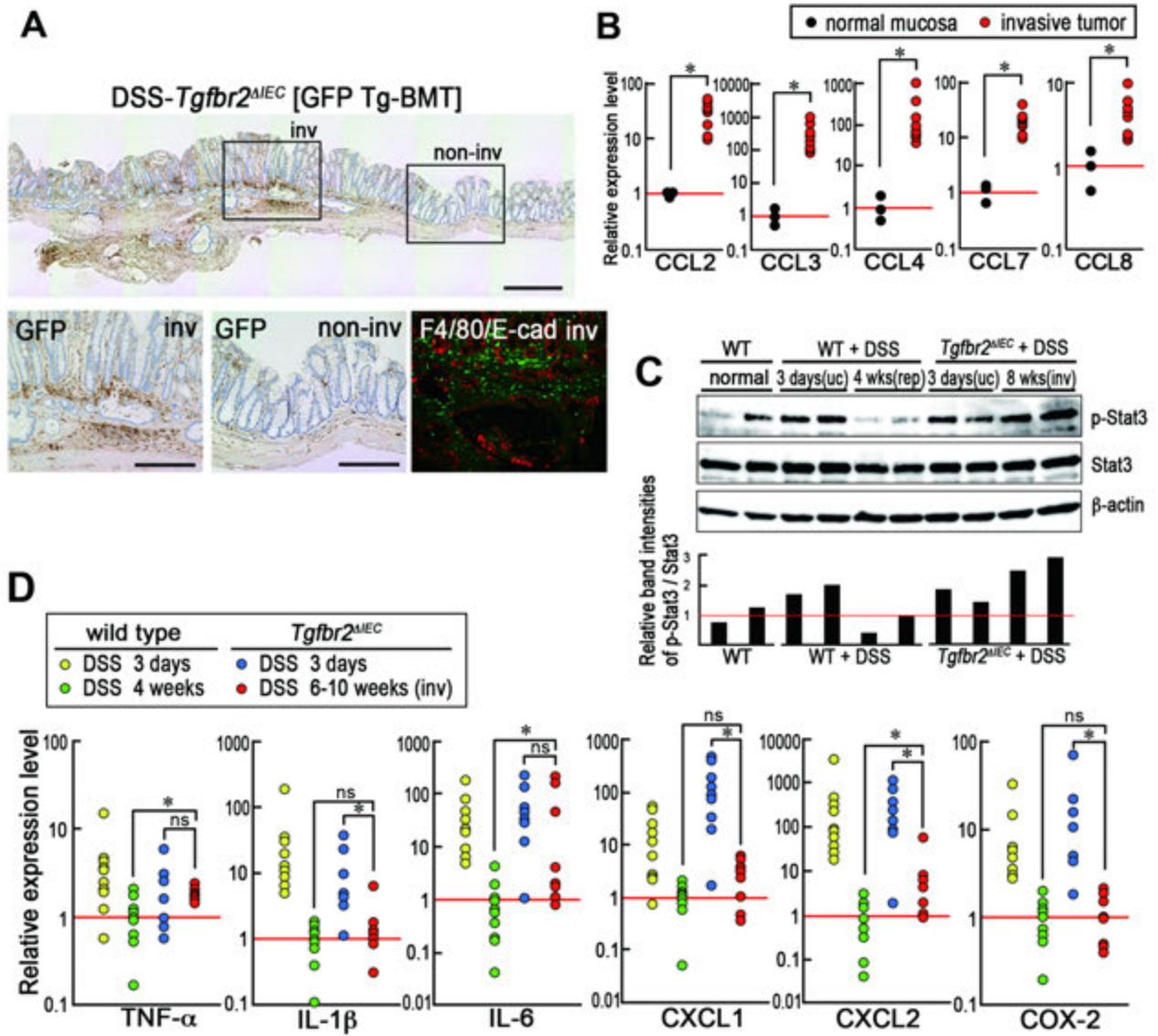


Figure 4

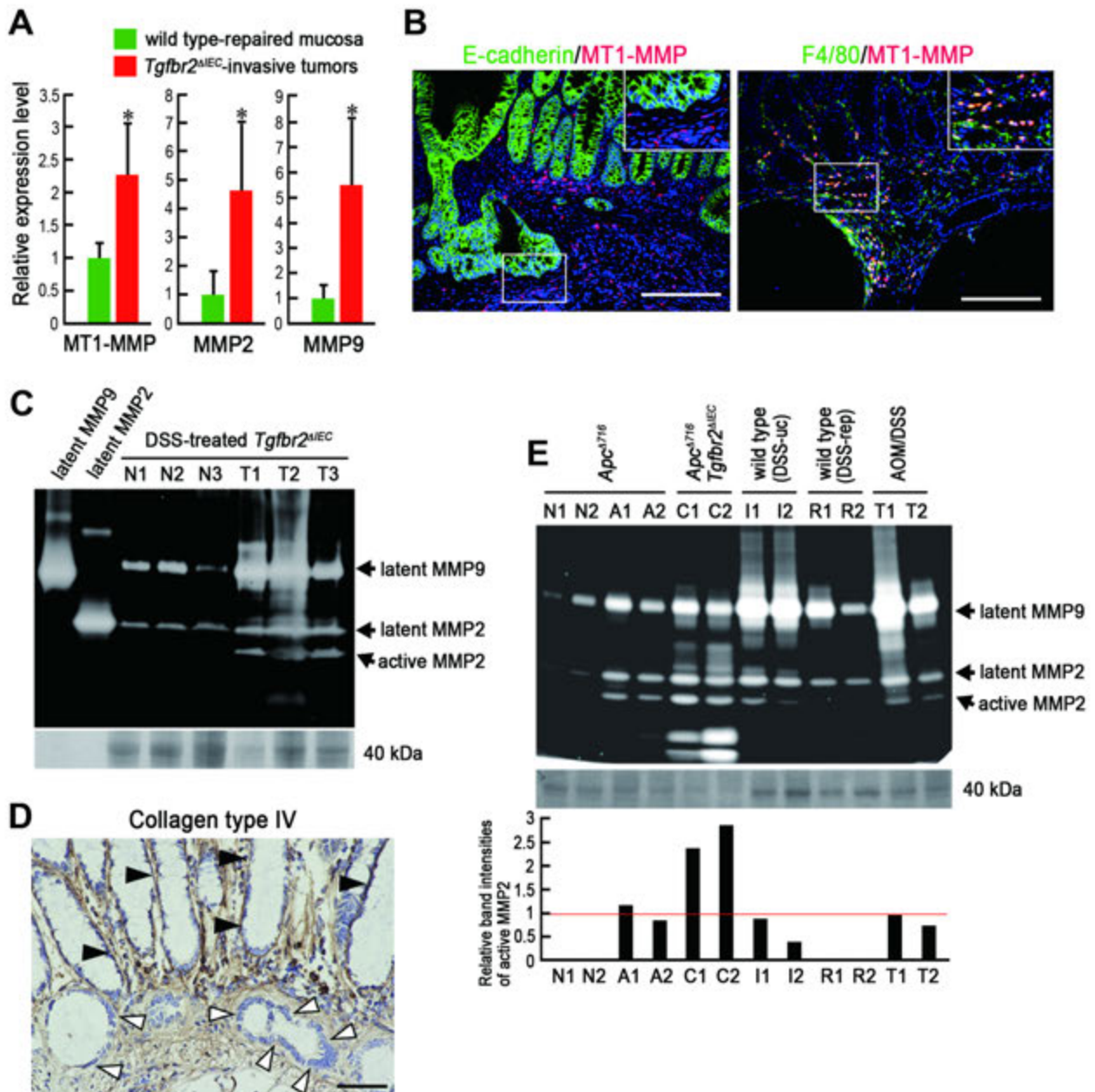


Figure 5

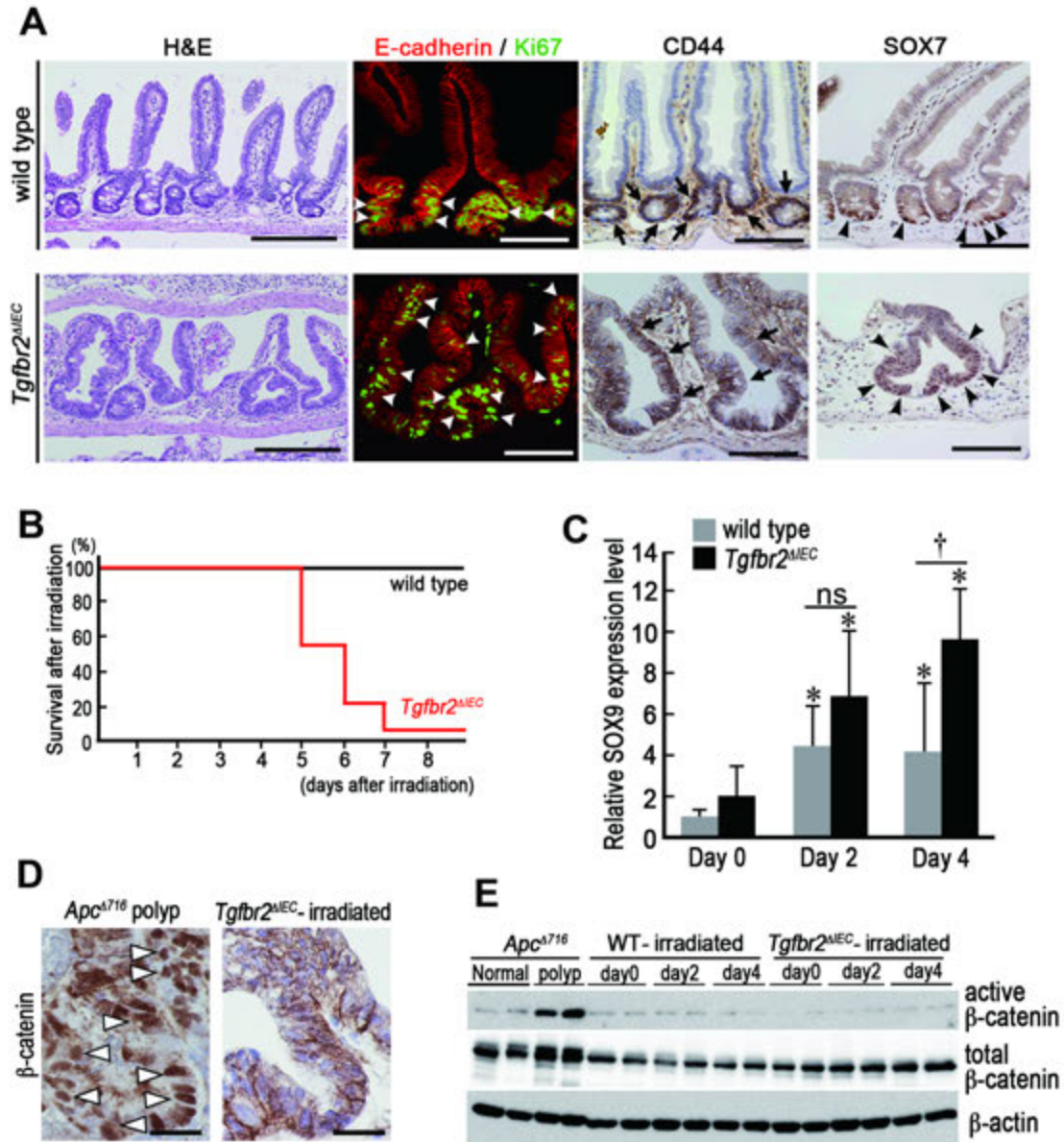


Figure 6

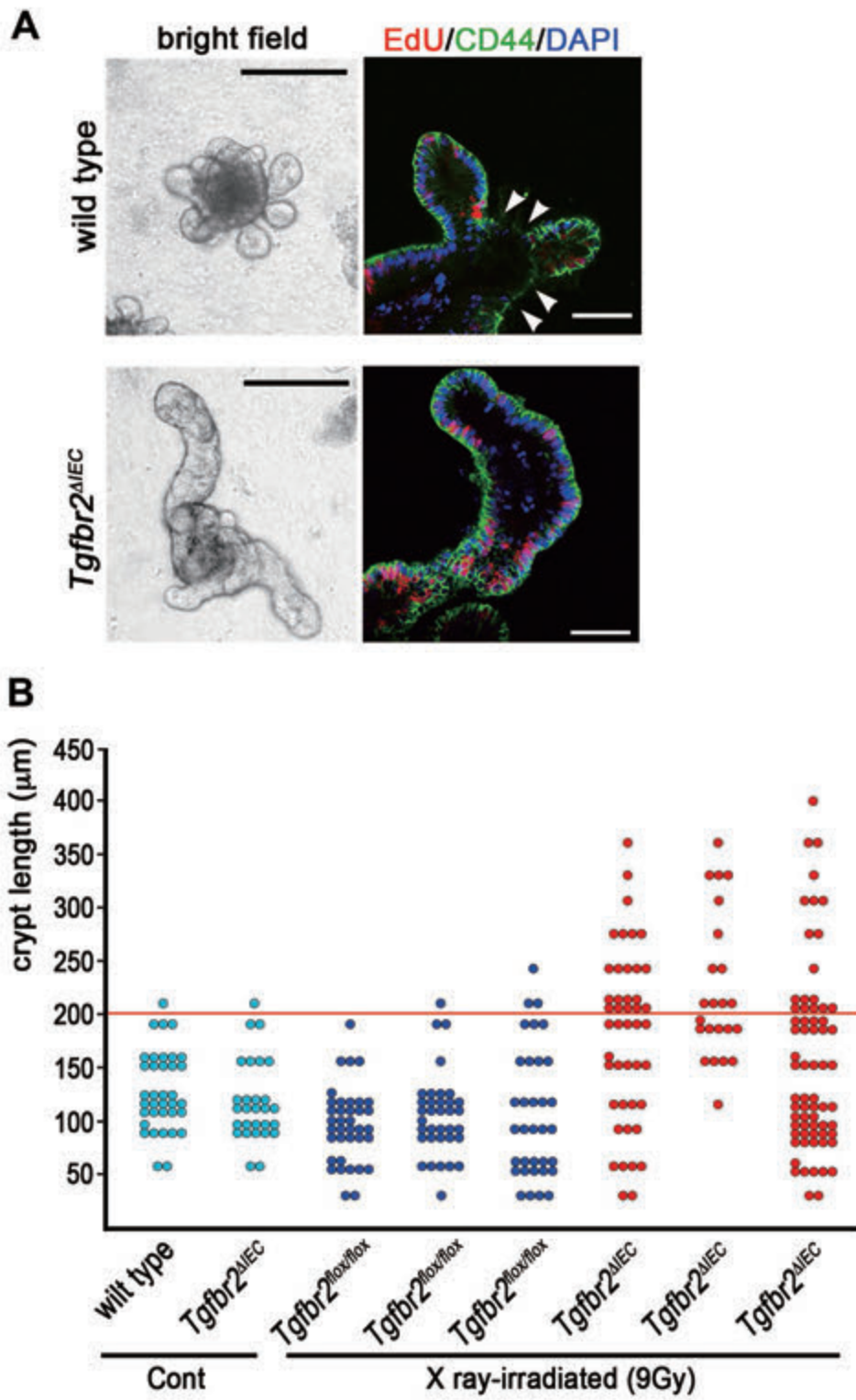


Figure 7

